

LUNAR BASALTS AND PYROCLASTIC DEPOSITS. SCIENCE AND RESOURCE TREASURES DELIVERED FROM THE MOON'S INTERIOR. C. K. Shearer^{1,2}, L. E. Borg³, and L. R. Gaddis⁴. ¹Institute of Meteoritics, Department of Earth and Planetary Science, University of New Mexico, Albuquerque NM, ²Lunar and Planetary Institute, Houston, TX 77058 (cshearer@unm.edu), ³Lawrence Livermore National Laboratory, Livermore CA 94550, ⁴Astrogeology Science Center, USGS, Flagstaff, AZ 86001.

Introduction. Lunar volcanic deposits cover less than 20% of the surface of the Moon and constitute less than a few percent of the crust [1]. Although they make up only a small volume of the lunar crust, they are scientifically significant because they are physical samples derived from melting of the lunar mantle. As such, volcanic deposits are probes of the lunar interior and provide a valuable record of the thermal state, composition, volatile abundance, age, and origin-evolution of the Moon. Furthermore, they define a critical link between mantle processes and their expressions on the lunar surface. Few differences are so great as those observed between the abundance of maria on the near side and on the far side of the Moon [e.g., 2-4]. Near-side maria are wide-spread, diverse, and span a range of ages [e.g., 3-5], whereas far-side maria are few, spotty, and occur primarily in South Pole-Aitken (SPA) basin (Fig 1) [2,6]. Maria in the SPA [2] were largely erupted in the Late Imbrian Period. Significantly younger maria are rare [7], in contrast to the younger maria that are abundant on the near side [e.g., 4,5]. Volatile-driven pyroclastic deposits are associated with the maria in SPA. More ancient basalts (cryptomaria) are abundant in the SPA region [5,8].

Basalts derived from the lunar far side provide a contrasting perspective of the evolution of the Moon (e.g., magmatic style, timing, extent of primordial differentiation). In addition, pyroclastic deposits are potential resources for human surface activity [e.g., 9-14].

Proximity of mare deposits to the South Pole (SP). The area within 3° of the SP is not the ideal location to examine basaltic volcanism. Orbital data has documented mare basalt, cryptomaria, and pyroclastic deposits Moon-wide and their proximity to the South Pole (Fig. 1). The closest mare and crypto-mare deposits are in the southern portions of SPA (-60° to -75°). The pyroclastic deposit in closest proximity to the SP is in Schrödinger basin (~-75°, 132.4°). Basalts that could be sampled by Artemis are those transported by impact processes or through robotic missions enabled by the Artemis architecture. Remnants of basaltic magmatism derived from adjacent terrain are likely to be in the regolith and breccias in the SP region. For example, at the A-16 site which is approximately 220 km from the nearest basalt flows the regolith contains 6% mare fragments [15]. Pyroclastic glasses have been identified in the regolith from all Apollo sites [16,17].

Ancient basalts have been identified in numerous clast-rich breccia returned by Apollo and may be analogous to lithologies in the outer portion of the SPA basin.

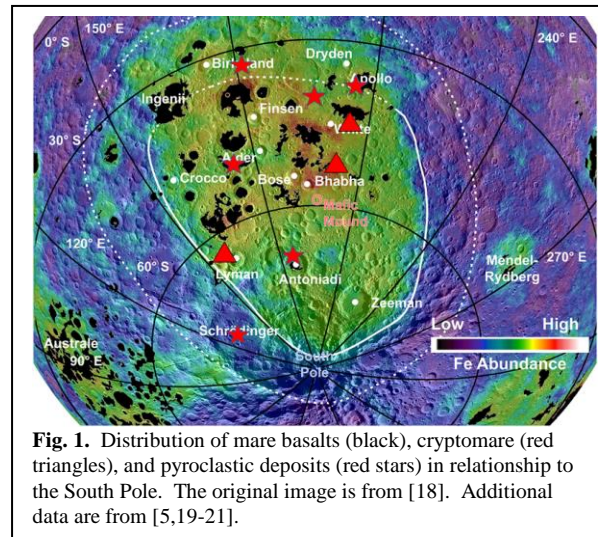


Fig. 1. Distribution of mare basalts (black), cryptomaria (red triangles), and pyroclastic deposits (red stars) in relationship to the South Pole. The original image is from [18]. Additional data are from [5,19-21].

Science Value. As probes of the lunar interior, basalts derived from the mantle outside of the influence of PKT provide important contrasts that will allow fundamental questions concerning the origin and evolution of the Moon to be addressed:

1. Distribution of basaltic volcanism: The dichotomy of the abundance and duration of mare volcanism on the Moon's far side versus near side has been attributed to the (a) lateral and (b) vertical distribution of radioactive elements in urKREEP (K, U, Th), and (c) the lateral asymmetry of the lunar crust which may act as an impediment to the eruption of mantle-derived magmas on the far side. These three hypotheses have significant implications for the early differentiation of the Moon, origin and nature of lateral asymmetry in the Moon's mantle, and its relationship to the distinct crustal asymmetry. Detailed chemistry, and mineralogy as well as experimentally determined depth of origin of far-side basalts will differentiate these hypotheses.

2. Heterogeneity of lunar mantle volatiles: Testing the models above provide insight into the nature and origin of mantle heterogeneity between the far-side and the near-side mantle, and its relationship to crustal heterogeneity. Analysis of the abundance and isotopic composition of volatile elements in far-side volcanics will allow identification of volatile reservoirs in the Moon's far-side mantle.

3. Ancient basaltic magmatism: The largest pulse of magma production occurred in the late Imbrian at 3.6 to 3.8 Ga [3-6]. A fundamental feature of the flux of basaltic magmas is that prior to the 3.6–3.8 pulse the eruptive flux appears to decline. There are several interpretations for the apparent decrease in eruptive flux prior to the 3.8 Ga peak: (a) little to no basalt volcanism prior to 3.8 Ga, (b) a gradual increase in magmatism from primordial lunar crust formation to 3.8 Ga, or (c) a rapid increase following lunar crust formation and it continued at the same rate through 3.8 Ga. Distinguishing among these models is difficult due to the older volcanic deposits being obscured by younger crater and basin-forming events. Chronology and geochemistry of cryptomare that reside in the SPA basin and potential accessible in clast-rich breccias in the SP region would test these 3 models.

4. Thermal evolution of the Moon: The limited abundance and duration of mare volcanism and the apparent low-concentration of heat producing elements on the far-side of the Moon hint at the contrasting thermal histories for different parts of the Moon (e.g. PKT, lunar highlands). High P-T experiments for far-side mare basalts and volcanic glasses compositions will establish their depth of melting or ponding. Used in conjunction with indexes of crystallization, source region compositional characteristics, and chronology the thermal structure of the mantle and crust and how it evolved with time will be constrained.

5. Timing and extent of primordial differentiation: During the Apollo Program, samples and remotely collected data led to the lunar magma ocean (LMO) hypothesis [e.g., 23,24]. Various versions of LMO models advocate an early primordial melting of the Moon followed by a crystallization sequence that produced the source regions for the mare basalts, ferroan anorthosites (FAS) crust, and an LMO late-stage residual melt (urKREEP). These components were the sources for subsequent periods of magmatism (e.g., Mg-suite, mare basalts). Recent chronologic investigations on lunar samples have demonstrated that there is a preponderance of 4.3-4.4 Ga ages. These ages have been obtained for: (1) the source regions of the mare basalts, (2) FAS, (3) urKREEP, and (4) Mg-suite rocks [e.g., 25-27 and Borg and Shearer (this volume)]. All these measurements were completed on rocks obtained within the area sampled by the Apollo missions on the lunar near side. The relatively young ages determined for these samples have been interpreted in several ways. The simplest explanation is that they record the primordial differentiation (i.e. LMO) [25,27]. A more complex explanation is that the 4.3 to 4.4 ages record a regional geologic event effecting the crust and mantle of the PKT region that occurred after LMO solidifica-

tion (e.g., large impact, post-LMO cumulate overturn) [28-30]. Samples of basalts from outside the PKT would (a) provide an unambiguous interpretation of this 4.3-4.4 Ga event (regional versus global), (b) establish the chronology of the LMO on the far side, and (c) define the extent and style of an LMO.

6. Lunar resources: Future work on pyroclastic deposits as potential resources would include sampling, identification, preservation, documentation of individual volcanic glasses in the regolith during human missions and exploring pyroclastic deposits robotically. Leaching and heating experiments of pristine returned samples, examination of the distribution of volatiles within deposits, and thermodynamic and dynamical modeling [31] will provide needed documentation to evaluate their potential as resources.

Surface capabilities to fulfill science goals: The astronauts must be trained to recognize these samples on the surface. Although analysis of mare basalt and pyroclastic glasses require small masses of material (100s g), individual clast-rich breccia samples may require a mass of ~5 to 12 kg. Particularly the latter would require a capability of returning upwards of 100 kg of material per SP mission. Sample diversity is important and addressing this will require (1) surface mobility similar to Apollo 17, (2) robotic exploration of areas outside the SP enabled by the Artemis infrastructure, (3) sampling regolith with depth. Finally, the capability of preserving volatile-rich mineral assemblages that could react with crew cabin and terrestrial environments (e.g., “rusty rock” 66095) would be invaluable. Current ANGSA studies will provide insights into sample containment systems [32].

References: [1] Head & Wilson (1992) *GCA* 56, 2155-2175. [2] Wilhelms, (1987) *The Geol. of the Moon* #1348. [3] Hiesinger & Head (2006) *RIMG* 60, 1-81. [4] Hiesinger et al. (2000) *JGR Planets* 105(E12) 29239-29275. [5] Hiesinger et al. (2011) *Rec. Adv. & Cur. Res. Issues in Lunar Strat.*, 477, 1-51. [6] Yingst and Head (1999) *JGR Planets* 104(E8) 18957-18979. [7] Haruyama et al. (2009) *Science* 323, 905-908. [8] Pieters et al. (2001) *42nd LPSC* #2173. [9] Gibson & Johnson, (1971) *2nd LSC* 1351. [10] Allen et al. (1996) *JGR Planets*, 101(E11), 26085-26095. [11] Taylor & Martel (2003) *Adv. in Space Res.* 31(11), 2403-2412. [12] Anand et al. (2012) *Planet. & Space Sci.* 74(1), 42-48. [13] Zacny et al., (2008) *AIAA SPACE 2008* p. 7824. [14] Sanders and Larson, (2012) *Earth & Space 2012*, 457-478. [15] Korotev (1997) *MAPS*, 32, 447-478. [16] Delano (1982) *13th LPSC* 27-28. [17] Shearer & Papike (1993) *GCA* 57, 4785-4812. [18] Moriarty & Pieters (2018) *JGR Planets* 123(3) 729-747. [19] Pieters et al. (2001) *JGR Planets* 106(E11), 28001-28022. [20] Bennett et al. (2016) *Icarus* 273, 296-314. [21] Besse et al. (2014) *JGR Planets*, 119(2), 355-372. [22] Shearer et al. (2006) *RIMG* 60, 365-518. [23] Smith et al. (1970) *1st LSC*, 897-925. [24] Wood et al. (1970) *1st LSC*, 965-988. [25] Borg et al. (2011) *Nature* 477, 70-72. [26] Borg et al. (2015) *MAPS* 50, 715-732. [27] Borg et al. (2019) *EPSL* 525. [28] Wicczorek & Phillips (2000) *JGR Planets* 105(E8), 20417-20430. [29] McLeod et al., (2014) *EPSL* 396, 179-189. [30] Shearer et al. (2015) *Am. Min.* 100, 294-325. [31] Renggli et al. (2017) *GCA* 206, 296. [32] Shearer et al. (2020) *51st LPSC*, #1181.